ARCHIVES OF ACOUSTICS
1, 2, 87-108 (1976)

NOISE AND STRUCTURE OF A GAS JET AT THE CHOKED OUTFLOW FROM A PERFORATED DISK

WIKTOR M. JUNGOWSKI, WITOLD C. SELEROWICZ
Department of Aerodynamics, Warsaw Technical University (Warszawa)

With the aid of experimental and theoretical investigations the main gasodynamic and acoustic properties of a gas jet discharging from a disk have been determined, and the range of efficient operation of the disk, as an element that reduces the outflow noise, has been established. The properties of the gas jet from a disk and a nozzle were compared.

Notation

c sound speed,
A cross-sectional area,
b distance between holes of the disk,
d diameter of hole or nozzle,
f frequency,
G_* critical mass rate of flow,
k ratio of specific heats,
L length of cell, $\overline{L} = L/d$,
M Mach number,
n number of holes,
n_h number of hexagons,
SPL overall sound pressure level,
p pressure, $\overline{p}_a = p_a/p_o$, $\overline{p}_{as} = p_a/p_{os}$, $\overline{p} = p_n/p_o$,
St Strouhal number,
u gas velocity, $\overline{u} = u_n/c_o$,
α ratio of cross-sectional areas,
$\beta = \sqrt{M^2 - 1}$,
$\eta = b/d$,
θ angle of direction between the jet axis and a radius (in horizontal plane) from the front of the nozzle or disk,
ϱ mass density.

Suffixes

a ambient conditions,
d nozzle,
g conditions on the boundary jet,
n supersonic jet,
o supply conditions,
p subsonic jet,
s substitute conditions in coalesced jet,
$*$ critical conditions.

1. Introduction

The investigation of perforated disks, as elements to reduce exhaust noise [5], has prompted the authors to devote themselves particularly carefully to the patterns of flow and the noise generated at a choked outflow for a wide range of supply pressure. Various structures of the coalesced jet and various noise spectra were found to exist. As a result of the investigations some properties of the coalesced jet and their dependence on the supply pressure have been established and this, in turn, has contributed to determining the efficient ranges of operation for disks of different geometries. In addition, the properties of the coalesced gas jet discharged from a disk and those of a jet from single convergent nozzle have been compared.

2. Gas jet at the choked outflow of a convergent nozzle

To enable the comparison of a coalesced jet from a disk with a jet from a nozzle to be made, it will be advisable to sum up and to analyze the essentials of the information contained in numerous publications, as well as the conclusions that result from the investigations of a single jet.

The gas jet at a choked outflow, while expanding outside the nozzle, forms a characteristic cell structure. The structure of cells, their dimensions and the shape of the shock waves encountered, depend on the ratio of the ambient pressure to the supply pressure [12, 6]. Fig. 1 shows our own photographs of a gas jet, obtained by a schlieren method, with the aid of the light from a mercury lamp. It can be seen that, as the supply pressure increases, the length of the cells is also increased (a, b), and there then appears a Mach disk in the first cell (c) and, subsequently, in the second (d). The empirical formulae of various authors for the length of the first cell (at the nozzle) for air discharge ($k = 1.4$) are presented below in a uniform notation. Two groups of formulae are remarkable: the first is characterized by simple relations with regard to $\overline{p}_a$

$$\bar{L} = 0.89\sqrt{\frac{1}{\overline{p}_a} - 1.9}, \quad [12], \text{ p. 74}, \tag{1}$$

$$\bar{L} = 1.55\sqrt{\frac{0.528}{\overline{p}_a} - 1}, \quad \text{when } 0.528 \geqslant \overline{p}_a \geqslant 0.264, \ [6], \tag{2}$$

$$\bar{L} = 1.52\left(\frac{0.528}{\overline{p}_a}\right)^{0.437} - 0.5, \quad \text{when } \overline{p}_a < 0.264, \ [6], \text{ p. 6}, \tag{3}$$

$$\bar{L} = 1.2\sqrt{\frac{1}{\overline{p}_a} - 1.89}, \quad [11], \text{ p. 1048}, \tag{4}$$

$$\bar{L} = 0.89\left(0.1 + \frac{0.317}{\overline{p}_a}\right)\sqrt{\frac{1}{\overline{p}_a} - 1}, \quad \text{when } 0.528 \geqslant \overline{p}_a \geqslant 0.352, \ [7], \tag{5}$$

$$\bar{L} = 0.89\sqrt{\frac{1}{\bar{p}_a} - 1}, \quad \text{when } \bar{p}_a < 0.352, \quad [7], \text{ p. 234}, \tag{6}$$

and the second by linear relationships to β

$$\bar{L} = 1.1\beta, \quad [2], \text{ p. 576}, \tag{7}$$

$$\bar{L} = 1.306\beta, \quad [1], \text{ p. 216}, \tag{8}$$

where

$$\beta = \sqrt{M^2 - 1} = \sqrt{5\left(\frac{1}{(\bar{p}_a)^{2/7}} - 1\right) - 1}.$$

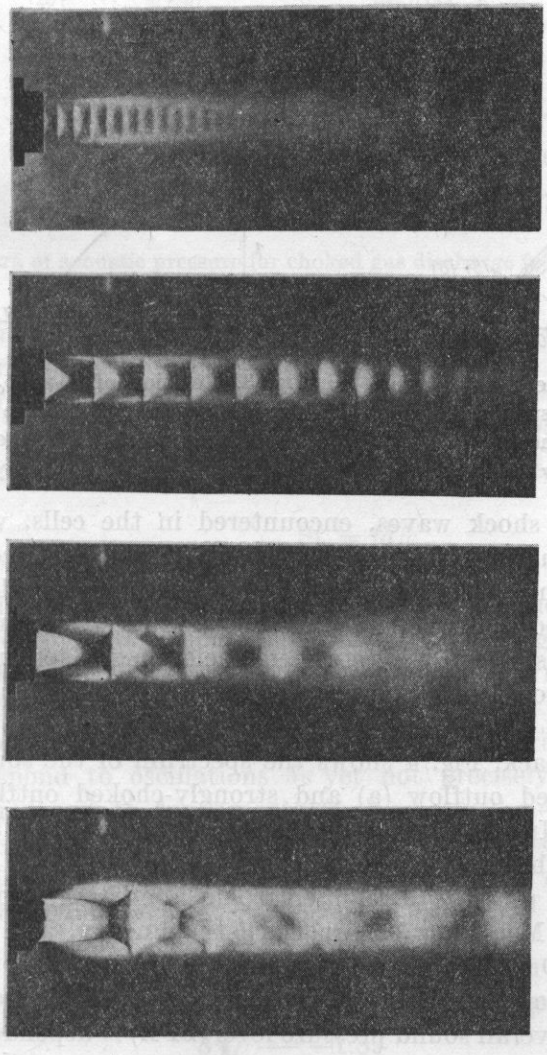

Fig. 1. Choked gas discharge from the nozzle

The results of computations made using the foregoing formulae are given in Fig. 2, where the results of the measurements of the cells' length from our own photographs are also plotted.

It can be seen that lengths of cells obtained from formulae (1), (4) and (7) differ considerably, whereas formulae (2) and (3), (5) and (6) as well as (8) differ by only a little and do not depart much from the results of measurements made by the present authors. For this reason the value of the ratio of the length of the cells over $\bar{p}_a$, obtained by measurement, has been found to be the most reliable and has provided the basis for plotting the graph $\bar{L}(\bar{p}_a)$ (Fig. 3). This, in turn, has found an application in the analysis of the supersonic gas jet formed at the outflow from the disk.

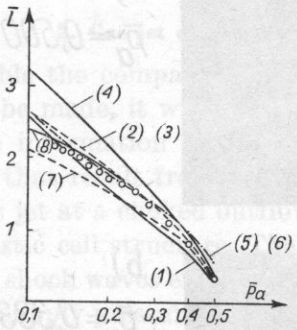

Fig. 2. Relation of the length of the first cell ($\bar{L}$) to the supply pressure ($\bar{p}_a$) of the nozzle
○ – measurements by the authors

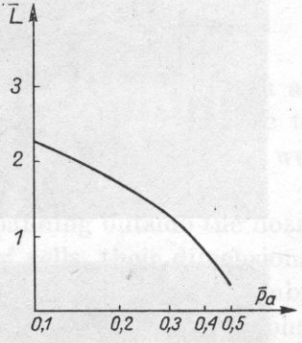

Fig. 3. Relation of $\bar{L}$ to $\bar{p}_a$ for the nozzle, according to the measurements of the authors

The interaction of shock waves, encountered in the cells, with vortices and turbulence in the unevenly expanded supersonic jet, produces additional noise, in addition to the turbulent mixing noise also generated in subsonic jets. The noise connected with the cell structure exhibits two components [2]. The former is distinguished by discrete frequencies in its spectrum and the occurrence of acoustic-flow feedback at its generation [10, 11]; it is usually called screech or whistle. The latter has a wider band with a definite peak and is produced without feedback. Fig. 4 shows the spectrum of the sound level obtained for weakly-choked outflow (a) and strongly-choked outflow (b) from the convergent nozzle. In the latter case the discrete frequency (5.4 kHz) and its first harmonic can be distinctly seen.

The overall sound pressure level increases as both the supply pressure causing an increase of Mach number on the jet boundary, and the rate of gas delivery increase. On the basis of previous results [2] and our own measurements, it has been found that for $\theta = 90°$ and within the range $0.5 < \beta < 1$ ($0.46 > \bar{p}_a > 0.31$) the overall sound pressure level (SPL) is dependent on β^4, i.e.

$$SPL[\mathrm{dB}] = \mathrm{const} + 40 \log \beta. \tag{9}$$

For $\beta > 1$, *SPL* is almost constant in level.

The generation by the jet of the above-mentioned discrete frequencies in the noise spectrum depends primarily on the ratio of the ambient pressure to the supply pressure and on conditions for the reflection of acoustic waves in the environment of the nozzle and jet [3, 4, 8, 9, 13]. The occurrence of strong discrete frequencies is connected with the decay of the discharging jet over a considerably shorter path than when they are absent (Fig. 1c).

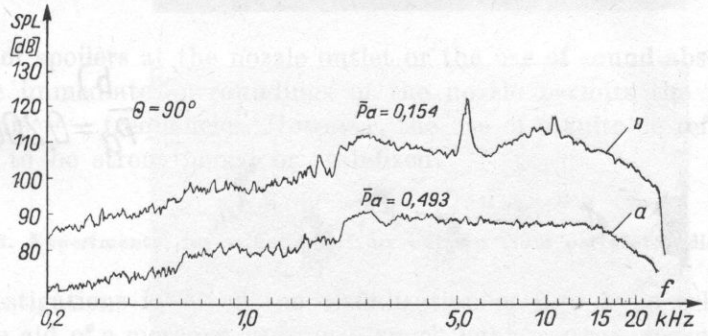

Fig. 4. Spectra of acoustic pressure for choked gas discharge from the nozzle for two values $\overline{p}_a$

Various forms of jet oscillations corresponding to different levels of supply pressure have also been described. It is possible to distinguish prevailing oscillations of an asymetric type [1, 4, 7-9, 11, 13], visible on photographs taken by schlieren (Fig. 5a) and shadow methods (Fig. 5b) using a spark light source. Fig. 6 compares Strouhal numbers evaluated from the formula

$$\mathrm{St} = fd/c_a \tag{10}$$

on the basis of the measurements of discrete frequencies stated in publications and obtained by the authors. It is possible to distinguish the band A throughout the whole range of $\overline{p}_a$ that corresponds to asymmetric oscillations, the band B within the range of higher values of $\overline{p}_a$ that correspond to oscillations of a symmetric type, and the band D within the range of lower values $\overline{p}_a$, that correspond to oscillations as yet not precisely investigated. The given values correspond to fundamental frequencies, whereas in spectra the first harmonic can frequently be observed. For comparison Strouhal numbers are also specified which have been evaluated from the empirical formulae stated in two publications:

$$\mathrm{St} = \frac{1}{3\sqrt{\frac{1}{\overline{p}_a} - 1.89}}, \quad [11], \text{ p. } 1048 \tag{11}$$

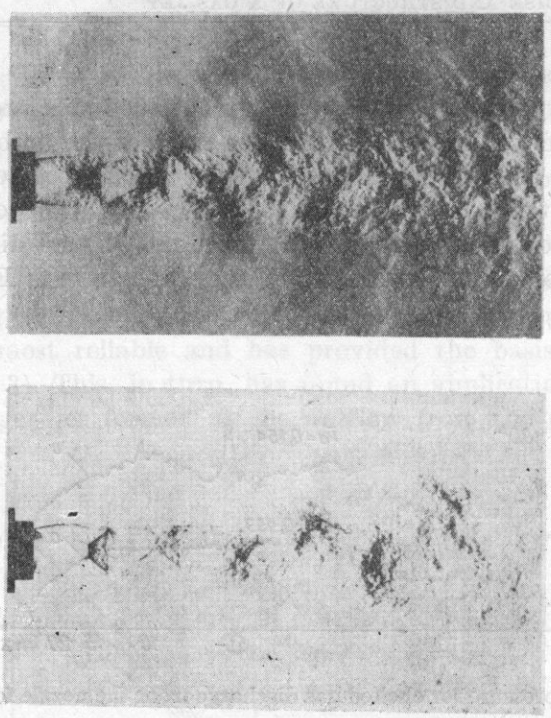

Fig. 5. Choked discharge from the nozzle-oscillations of the jet (of an asymmetric type): a) the photo made by steak trail method, b) the photo made by shadow method

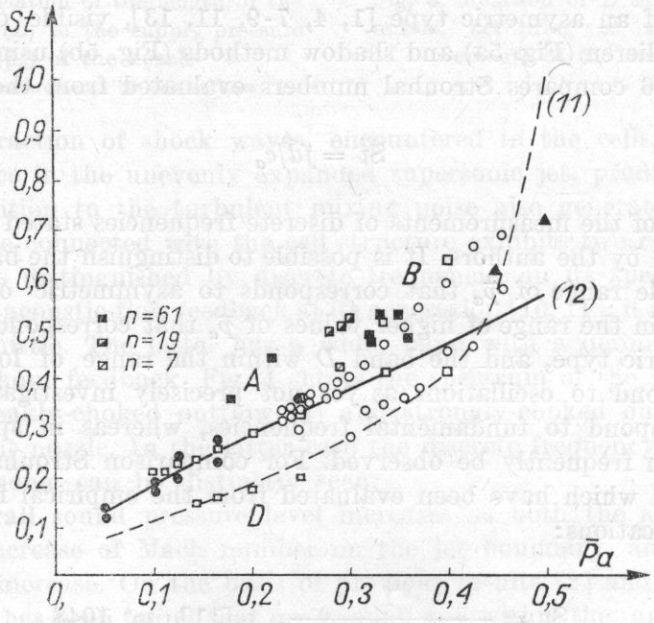

Fig. 6. Relation of Strouhal number to supply pressure ($\bar{p}_a$) for discrete frequencies in a spectrum

■ – measurements by the authors

and

$$\mathrm{St} = \frac{0.567}{\sqrt{\frac{1}{\overline{p}_a} - 1}}, \quad [7], \text{ p. } 235. \tag{12}$$

It can be seen that formula (12) is in a good agreement with the measurement results within a wide range of $\overline{p}_a$ and is associated with the band A. On the other hand, formula (11) is only partially in agreement with all three bands.

The use of spoilers at the nozzle outlet or the use of sound-absorbing materials in the immediate surroundings of the nozzle permits the removal of some of the discrete frequencies. However, the use of a suitable reflector may enable them to be strengthened or stabilized.

3. Experimental investigation of air outflow from perforated disks

The investigations involved the visualization of flow by a schlieren method with the aid of a mercury lamp or a spark light source; measurements of static and stagnation pressure by means of a Prandtl tube of small dimensions; measurements of overall sound pressure level (*SPL*) and noise spectra with the aid of apparatus from Brüel and Kjaer comprising a half-inch microphone (type 4133) with pre-amplifier (type 2616), analyser (type 2010) and level recorder (type 2307). A microphone was located at a radius of 50 cm from the nozzle outlet or the disk, and the angle θ between the radius and jet axis in a horizontal plane varied within the range 45° to 135°.

All disks were provided with holes arranged on the sides of hexagons (Fig. 20a). The total cross-section of the holes was always equal to the cross-section of the nozzle, of diameter 16 mm. The number of holes in the disks depended on the number of concentric hexagonals and can be expressed by the formula [1]

$$n = 1 + 3n_h(n_h + 1). \tag{13}$$

Disks with three numbers of holes arranged at various distances were used:

n_h	n	η					
1	7	0.5	0.645				
2	19	0.07	0.5	0.861			
4	61	0.07	0.5	0.772	1.07	1.243	1.523

Visualization of jet structures. Figs. 7 and 8 show air jets discharging from disks with equal $\eta = 0.5$, but with different numbers of holes: 61 and 19, respectively. At lower supply pressures the cell structure occurs only in the prox-

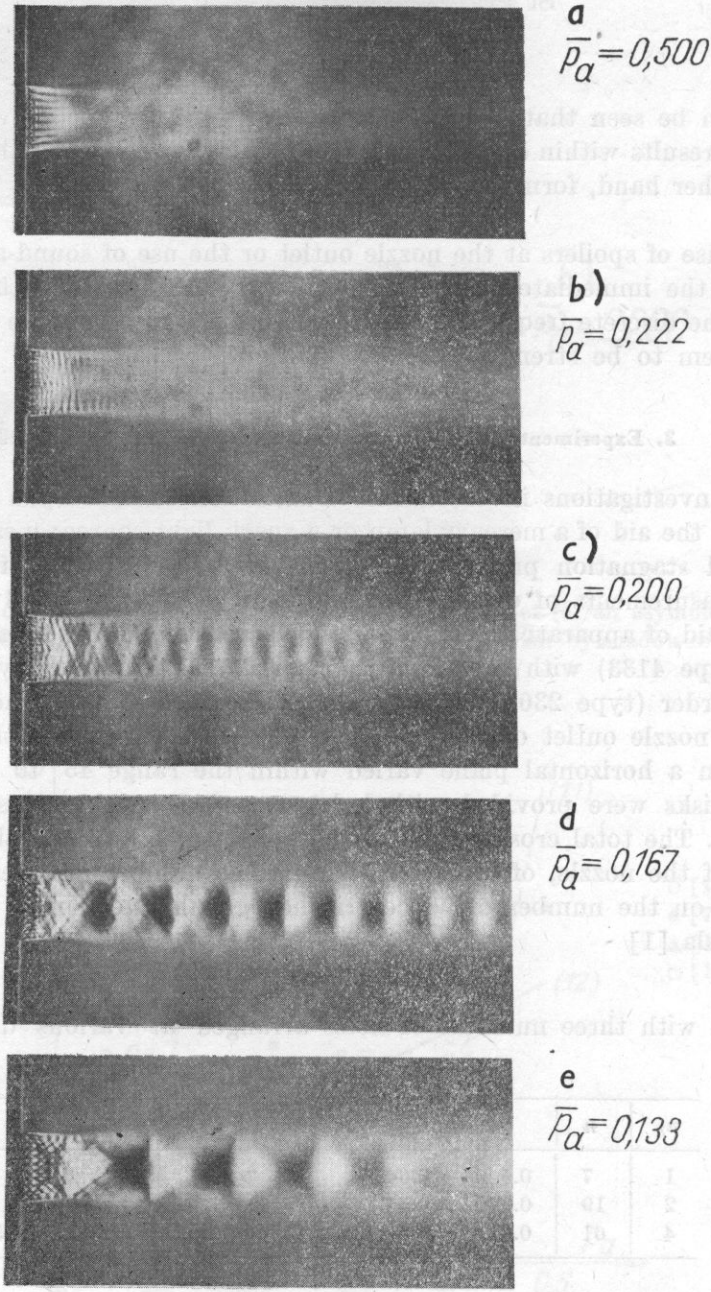

Fi .7. Choked gas discharge from a disk ($n = 61$, $\eta = 0.5$) for various supply pressures

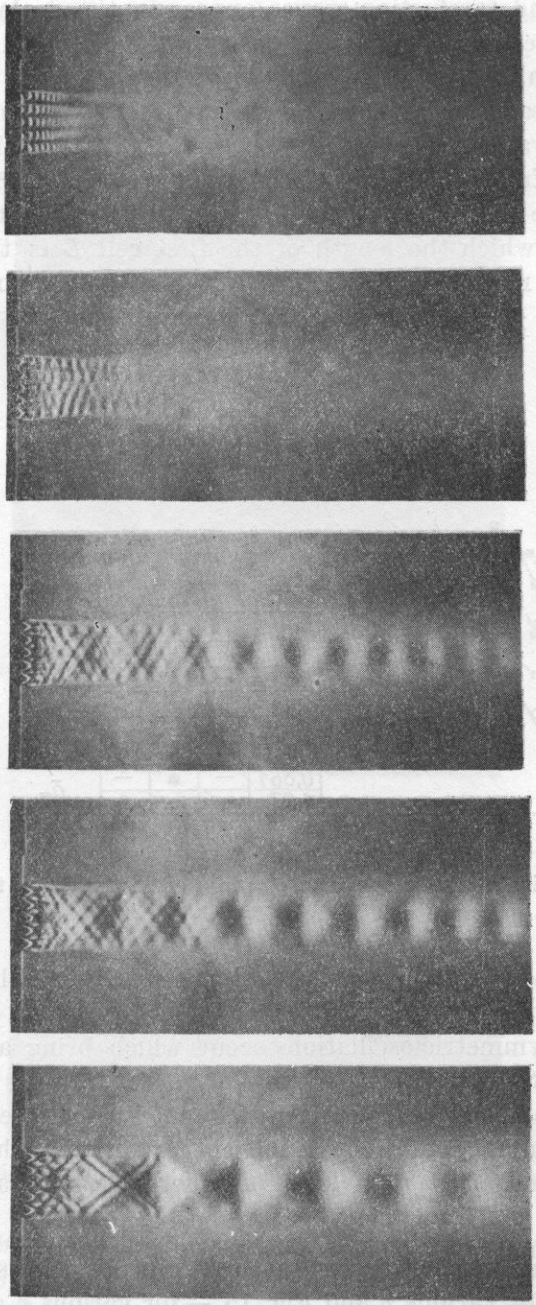

Fig. 8. Choked gas discharge from a disk ($n = 19$, $\eta = 0.5$) for various supply pressures

imity of the disk. Jets meet as subsonic ones to form a coalesced subsonic jet (a). As the pressure increases, the plane of joining of the jets moves towards the disk, while shock and rarefaction waves appear in the coalesced jet (b). With sufficiently high pressure distinct cells occur in the coalesced jet (c, d, e), which increase in length as the supply pressure rises.

On the basis of the measurement of the length of the first distinct cell of the coalesced jet and the graph shown in Fig. 3, the form of the substitute supply pressure ($\overline{p}_{as}$) as a function of real disk supply pressure ($\overline{p}_a$) is shown in Fig. 9 (the substitute disk supply pressure ($\overline{p}_{as}$) corresponds to the nozzle supply pressure ($\overline{p}_a$) at which the length of the first cell $\overline{L}$ is the same for both the disk and the nozzle). As can be seen, the growth of η at constant n and $\overline{p}_a$ causes $\overline{p}_{as}$ to increase, i.e. reduces the substitute supply pressure p_{os}.

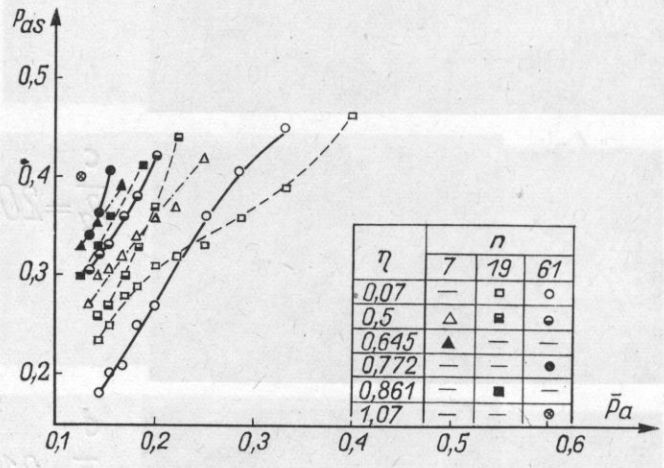

Fig. 9. Relation of the substitute supply pressure ($\overline{p}_{as}$) in a coalesced jet to the real supply pressure of the disk ($\overline{p}_a$)

Figs. 10-13 show gas jets at various supply pressures. At the lower and the higher values (a, c) the jet is stable and coherent, while at intermediate pressures (b) distinct asymmetric oscillations occur which bring about a very rapid decay of the jet. Such structures exist at various values of η and n. In the figures we can see Mach waves of high frequency which are propagating conically from the jet boundary, in the proximity of the disk. Furthermore, Fig. 13a shows acoustic disturbances of a lower frequency which are probably induced by oscillations of symmetric type.

Measurements of overall sound pressure level. Fig. 14 shows the dependence of the *SPL* on $\overline{p}_a$ for various η and Fig. 15 — for various n and angles θ. From Fig. 14 it can be seen that reduction in η at constant n causes a steep rise of *SPL* at lower supply pressures. This rise comes from the supersonic coales-

ced jet. Within a wide range of pressures the minimum level *SPL* is obtained for $\eta = 0.772$. Fig. 15 shows a reduction in *SPL*, within a wide range of pressures, as n increases with constant η. The increase of *SPL* to a level that corresponds to the *SPL* of the nozzle occurs at very similar values of the supply pressure.

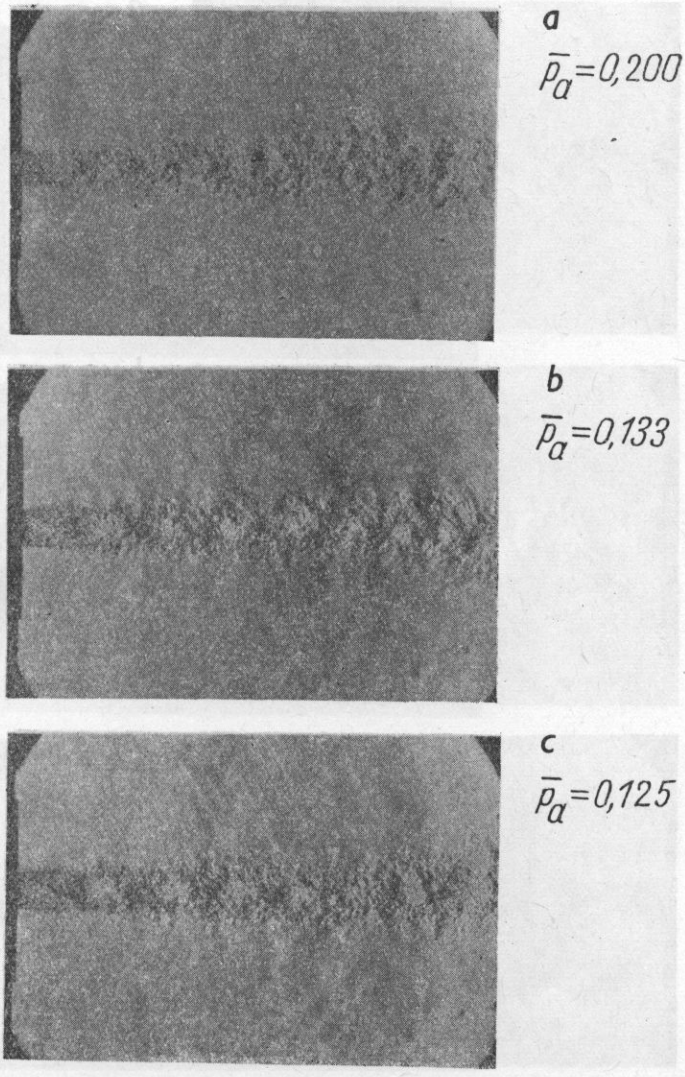

Fig. 10. Choked gas discharge from a disk ($n = 61$, $\eta = 0.07$)

The spectrum of acoustic pressure. Fig. 16 shows spectra obtained at three values of the supply pressure. The spectrum (a) corresponds to a subsonic coalesced jet, and (b) and (c) to a supersonic jet with cellular structure. The last two spectra both contain a distinct peak caused by broad-band noise

resulting from the cellular structure. Furthermore, in the spectrum (c) there occur two discrete frequencies that correspond to the noise induced by asymmetric flow oscillations with acoustic-feedback. The higher frequency is a first harmonic.

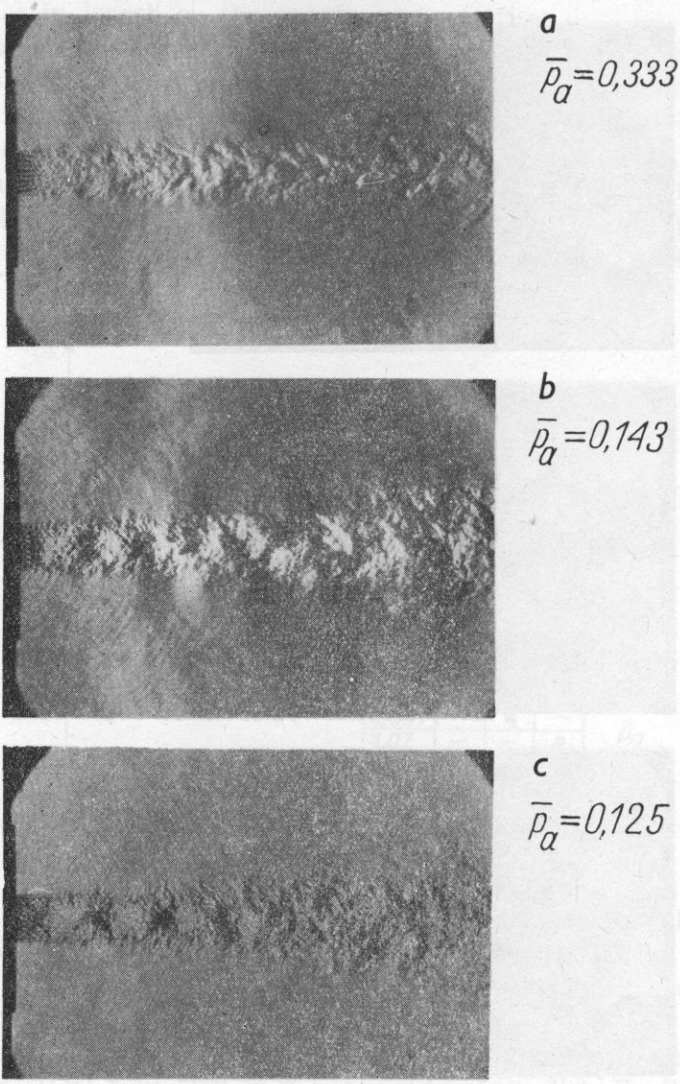

Fig. 11. Choked gas discharge from a disk ($n = 61$, $\eta = 0.5$)

Fig. 17 shows the results for the other disk. In the spectrum (c) one discrete frequency can be seen.

Fig. 18 and 19 show the effect of the angle θ on the shape of the spectrum, which, evidently, is negligible.

Measurement of stagnation and static pressures. The values of stagnations pressure as measured on the axis of the subsonic coalesced jet (in its initial cross-section) are plotted in Fig. 21a ($M_p < 1$). While measuring the static pressure at the beginning of the supersonic coalesced jet, a substantial excess

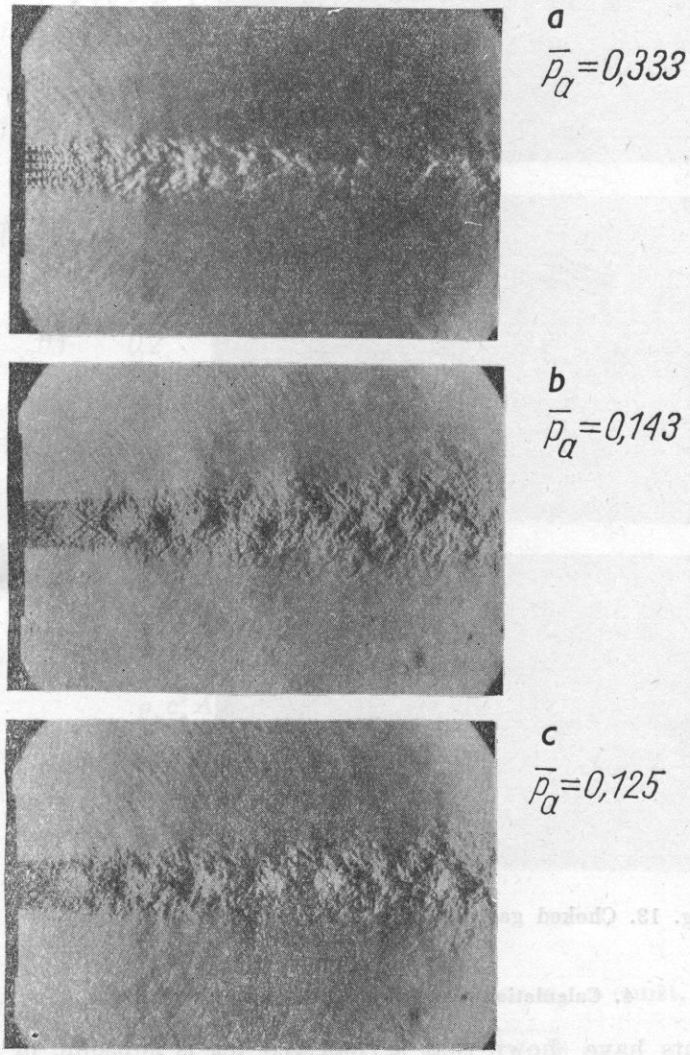

Fig. 12. Choked gas discharge from a disk ($n = 19$, $\eta = 0.5$)

pressure only a little below 1 atm at the maximum supply pressure was found to exist. The results have not been compared because they are few as a result of considerable air consumption during measurement at high supply pressures.

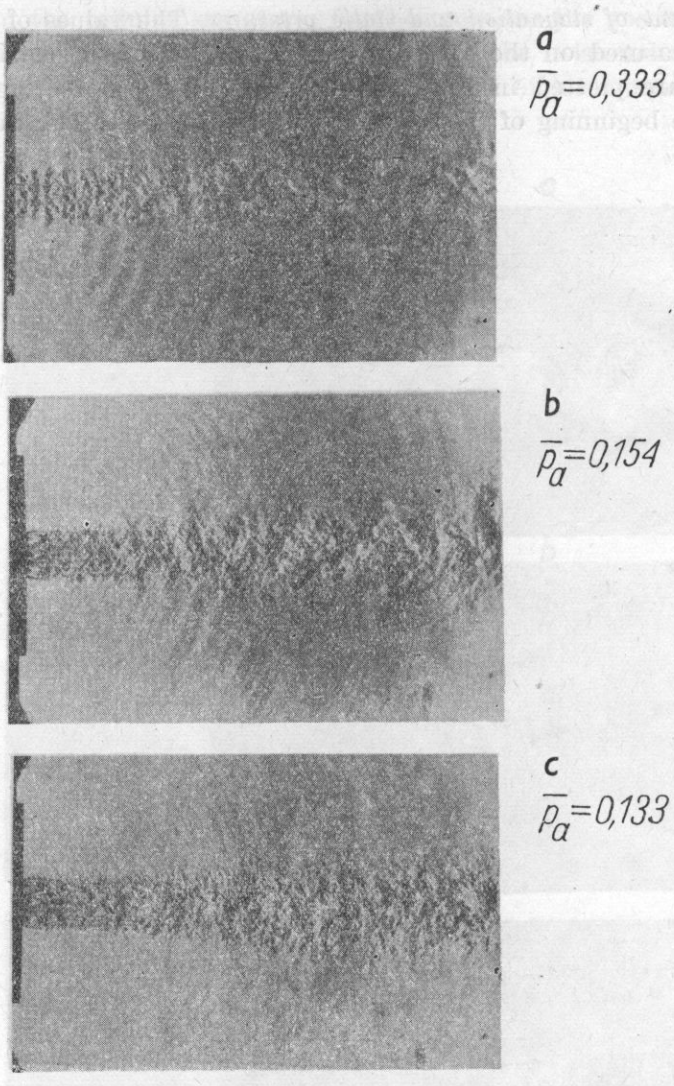

Fig. 13. Choked gas discharge from a disk ($n = 7$, $\eta = 0.5$)

4. Calculation the properties of a coalesced jet

Experiments have shown that a coalesced jet is subsonic or supersonic with cell structure depending on the range of $\bar{p}_a$, η and n. For this reason, physical models used for the calculation will be different for different jets. In both cases a simplifying assumption has been made that the gas properties at the initial cross-section of a collective jet are uniform.

Subsonic flow in a collective jet. A diagram of the structure of the flow is shown in Fig. 20b. Due to mixing of the jets discharging from a disk with

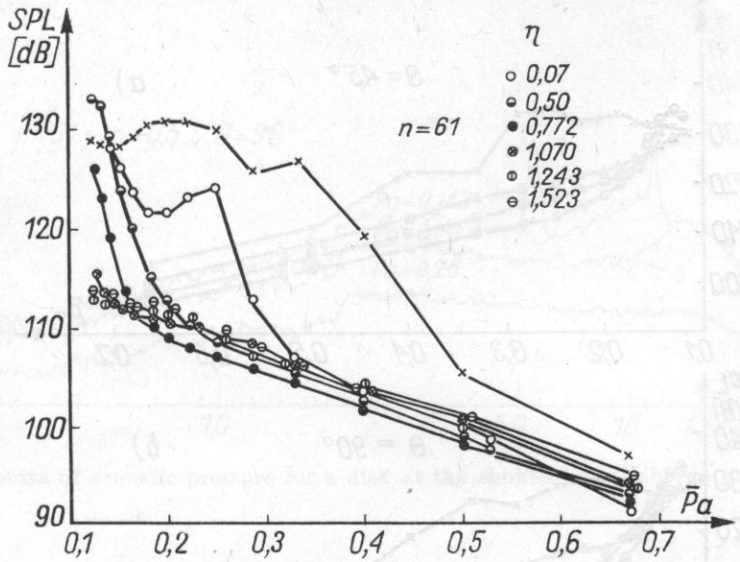

Fig. 14. Relation of *SPL* to $\bar{p}_a$ for various η ($\theta = 90°$) × – nozzle

the ambient air, subsonic portions of the jet develop around the decaying cell structure.

At a certain distance away from the disk they come into contact with each other and form a coalesced subsonic jet. Applying the principle of conservation of momentum to those jets we obtain:

$$\varrho_* c_*^2 A_* + (p_* - p_a) A_* = \varrho_p u_p^2 A_p. \tag{14}$$

After giving consideration to the equations of state of gas for single and coalesced jet, and relations

$$\alpha_p = A_*/A_p \tag{15}$$

and

$$M_p = u_p/c_p, \tag{16}$$

we determine the relation between M_p and $\bar{p}_a$, for $\alpha_p = \text{const}$, in the form

$$M_p = \sqrt{\frac{\alpha_p}{k}\left[\frac{2}{\bar{p}_a}\left(\frac{2}{k+1}\right)^{1/(k-1)} - 1\right]}. \tag{17}$$

With the aid of tables for isentropic gas flow we may find $\bar{p}_{as}(M_p)$.

It can be concluded from (17) that the problem involves a proper determination of α_p. The cross-section of the coalesced jet has been defined in two ways: as the total of the cross-sections of all of the jets with diameters

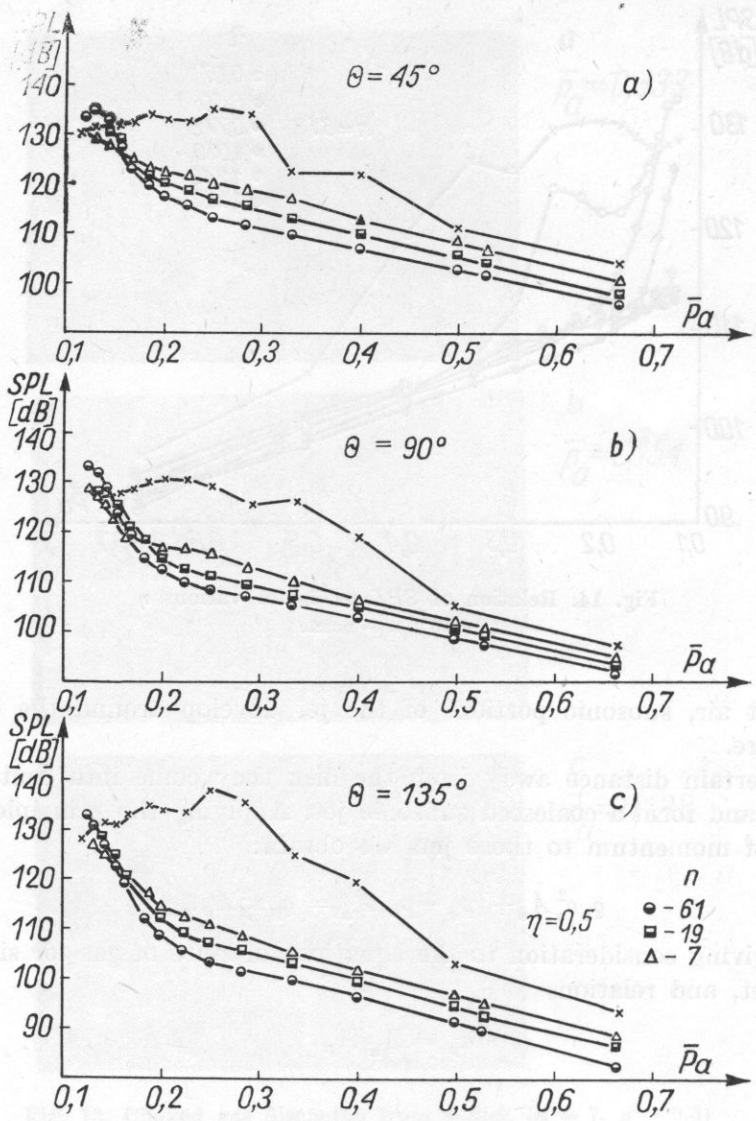

Fig. 15. Relation of *SPL* to $\overline{p}_a$ for various n and θ ($\eta = 0.5$)
× – nozzle

$d+b(A_{p1})$ or as the area (A_{p2}) bounded by dash-dot curve in Fig. 20a. Correspondingly, one obtains

$$a_{p1} = \frac{1}{(1+\eta)^2}, \tag{18}$$

$$a_{p2} = a_{p1} \frac{\pi[1+3n_h(n_h+1)]}{\frac{\pi}{6} + \frac{5}{\sqrt{3}} + 6n_h(\sqrt{3}n_h+2)}. \tag{19}$$

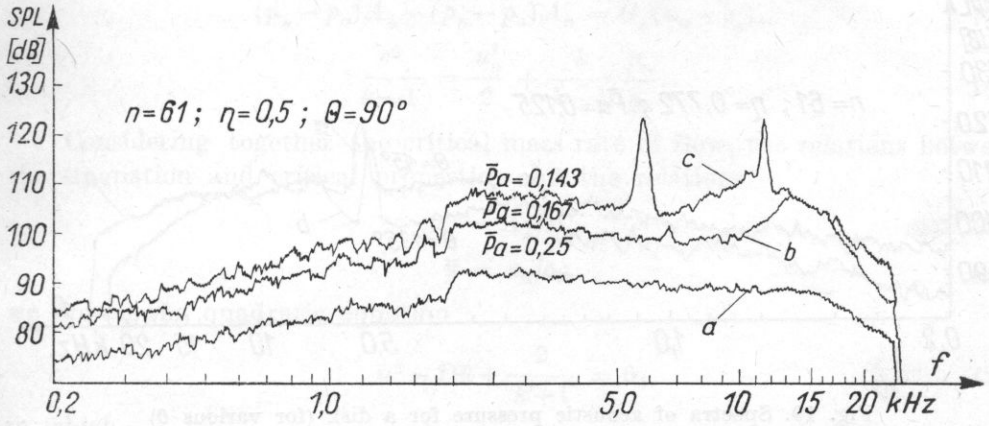

Fig. 16. Spectra of acoustic pressure for a disk at the choked gas discharge (for various $\overline{p}_v$)

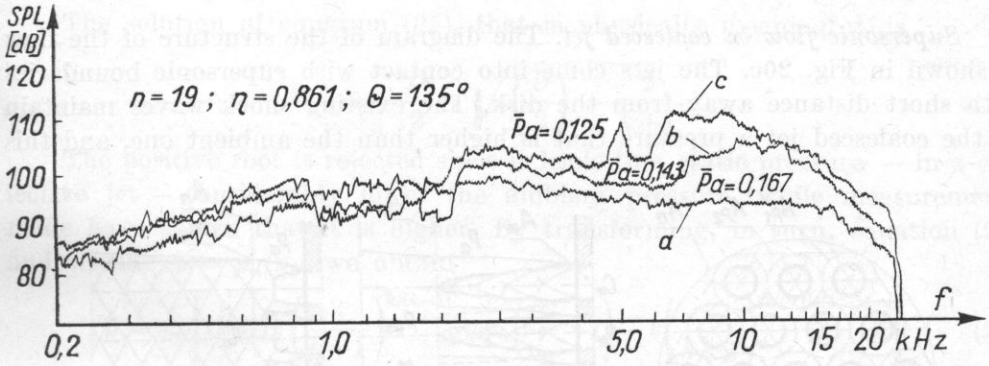

Fig. 17. Spectra of acoustic pressure for a disk (for various $\overline{p}_a$)

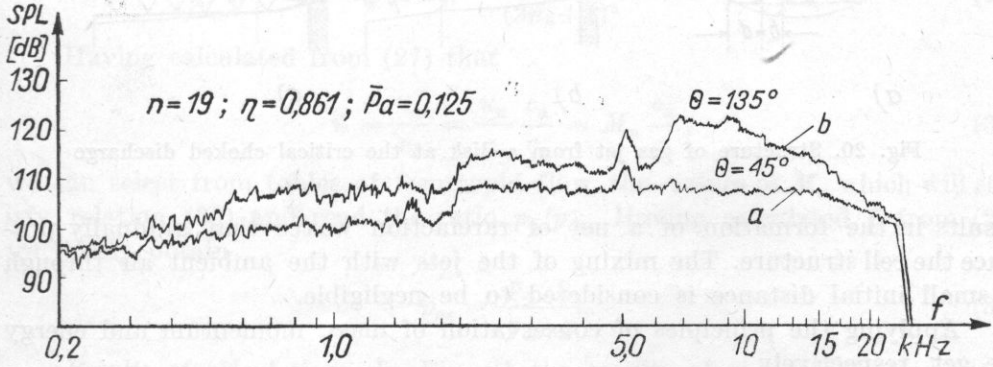

Fig. 18. Spectra of acoustic pressure for a disk (for various θ)

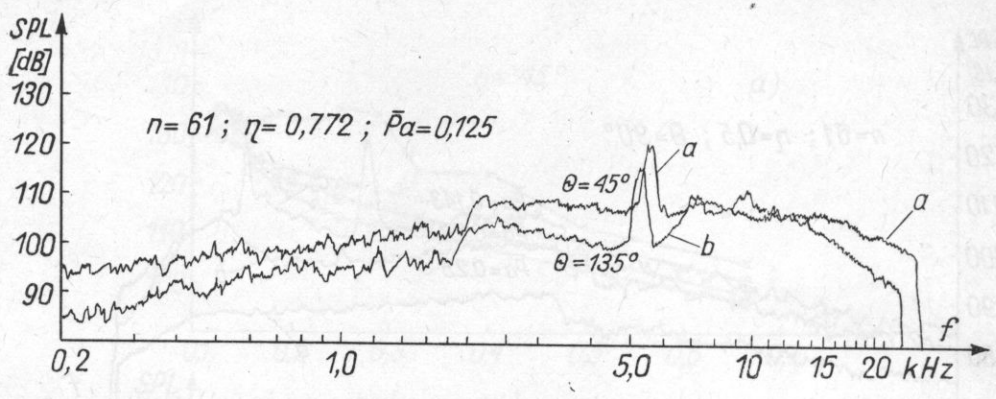

Fig. 19. Spectra of acoustic pressure for a disk (for various θ)

Thus α_{p1} depends only on the spacing of holes while α_{p2} depends also on their number.

Supersonic flow in coalesced jet. The diagram of the structure of the flow is shown in Fig. 20c. The jets come into contact with supersonic boundaries at a short distance away from the disk. The existing shock waves maintain in the coalesced jet a pressure that is higher than the ambient one, and this

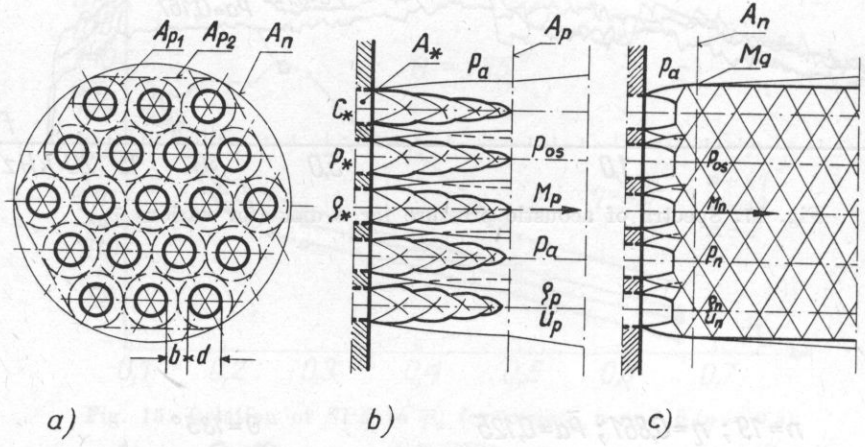

Fig. 20. Structure of gas jet from a disk at the critical choked discharge

results in the formation of a net of rarefaction waves that gradually produce the cell structure. The mixing of the jets with the ambient air through a small initial distance is considered to be negligible.

Applying the principles of conservation of mass, momentum and energy we get, respectively,

$$G_* = \varrho_n u_n A_n, \tag{20}$$

$$(p_* - p_a)A_* - (p_n - p_a)A_n = G_*(u_n - c_*), \tag{21}$$

$$\frac{c^2}{k-1} = \frac{u_n^2}{2} + \frac{k}{k-1}\frac{p_n}{\varrho_n}. \tag{22}$$

Considering together the critical mass rate of flow, the relations between the stagnation and critical properties and the relations

$$a_n = A_*/A_n, \tag{23}$$

$$\bar{u} = u_n/c_0, \tag{24}$$

we obtain the quadratic equation

$$\bar{u}^2 - D\bar{u} + \frac{2}{k+1} = 0, \tag{25}$$

in which

$$D = 2\left(\frac{2}{k+1}\right)^{1/2} + \bar{p}_a\left(\frac{1}{a_n} - 1\right)\left(\frac{2}{k+1}\right)^{(k-3)/2(k-1)}. \tag{26}$$

The solution of equation (25), that is physically meaningful, is

$$\bar{u} = \frac{D}{2} - \sqrt{\left(\frac{D}{2}\right)^2 - \frac{2}{k+1}}. \tag{27}$$

The positive root is rejected since it leads to a static pressure — in a collective jet — considerably lower the ambient pressure, while measurements made have shown that it is higher. By transforming, in turn, equation (21) and writing $\bar{p} = p_n/p_o$, we obtain

$$\bar{p} = a_n\left[(k+1)\left(\frac{2}{k+1}\right)^{k/(k-1)} + \bar{p}_a\left(\frac{1}{a_n} - 1\right) - k\left(\frac{2}{k+1}\right)^{(k+1)/2(k-1)}\bar{u}\right]. \tag{28}$$

The cross-section of the coalesced jet is defined as the circular area bounded by continuous line in Fig. 20a, which implies

$$a_n = a_{p1}\frac{1+3n_h(n_h+1)}{(2n_h+1)^2}. \tag{29}$$

Having calculated from (27) that

$$\bar{u} = \frac{u_n}{c_o} = \frac{u_n}{c_n}\frac{c_n}{c_o} = M_n\frac{c_n}{c_o}, \tag{30}$$

we can select from tables of isentropic flow the values of M_n which will satisfy relation (30) and read the ratio p_n/p_{os}. Having calculated $\bar{p}$ from (28) we finally obtain

$$\bar{p}_{as} = \frac{p_n}{p_{os}}\frac{p_a}{p}. \tag{31}$$

Results of calculations. In Fig. 21 the results of the calculations made using the above relations are denoted with continuous lines. For a subsonic

coalesced jet (a) ($M_p < 1$), the results of measurement show good agreement with the results of calculations obtained using α_{p1} for bigger η, and α_{p2} for smaller. In the case of a supersonic jet ($M_g > 1$) this agreement deteriorates, notably for $n = 19$.

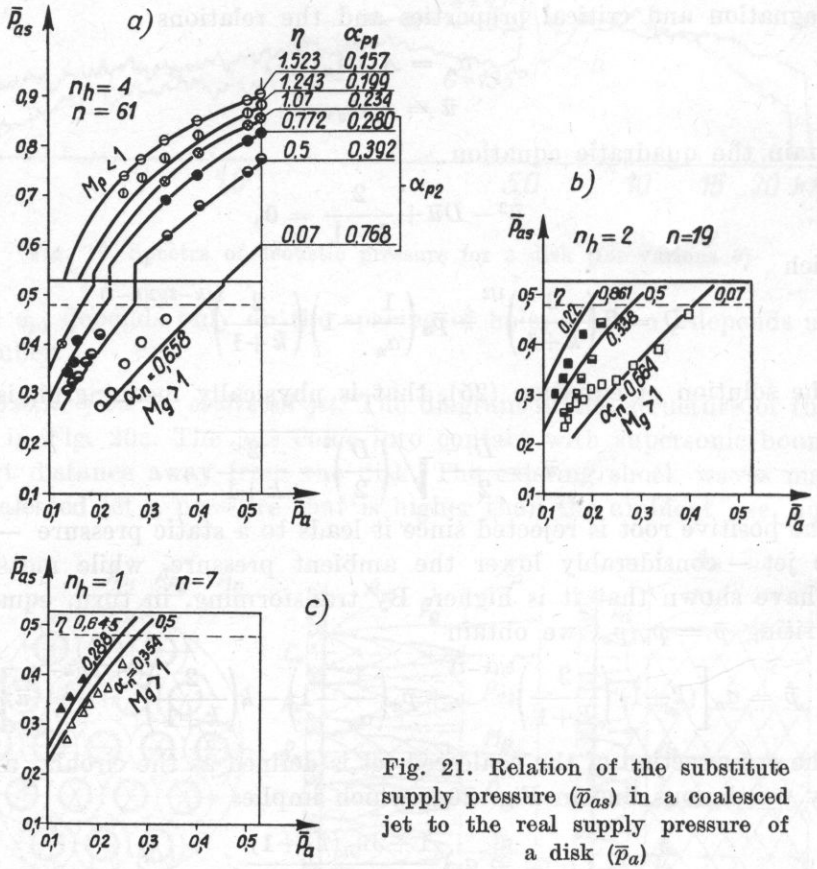

Fig. 21. Relation of the substitute supply pressure ($\bar{p}_{as}$) in a coalesced jet to the real supply pressure of a disk ($\bar{p}_a$)

The curves obtained do not join at $\bar{p}_{as} = 0.528$, i.e. when the flow in the coalesced jet is critical. In the transsonic range, measurement results are lacking but it might be supposed that they would not have been in agreement with the calculations. These facts result from the application of the two different models of flow which are correct for a subsonic or a supersonic coalesced jet.

5. Comparison of the jet from perforated disk with the jet from a nozzle

At the choked discharge of a gas from a perforated disk the collective jet can be subsonic, similar to subsonic discharge from a convergent nozzle, or supersonic, as for choked discharge. The nature of the structure of the

coalesced jet depends on the substitute supply pressure $\overline{p}_{as}$ which, in turn, is a function of $\overline{p}_a$, n and η. The collective jet exhibits all properties of the jet from a nozzle at corresponding supply pressures, i.e. when $\overline{p}_{as} = \overline{p}_{ad}$.

The *SPL* of the disk is linearly dependent on $\overline{p}_a$ since the coalesced stream is subsonic, as is the case for the disk in the range of subsonic discharge. When the cell structure appears, the *SPL* increases rapidly, as in the choked discharge from the nozzle, and can attain a level that corresponds to its maximum *SPL*.

The nature of the *SPL* spectra in corresponding supply pressure ranges is the same for the disk and nozzle. In the subsonic range the spectra are flat, while in the supersonic one they exhibit a distinct peak and discrete frequencies. Strouhal numbers calculated on the basis of discrete frequencies fall into the same range as they do for the nozzle if $\overline{p}_{as} = \overline{p}_{ad}$ (Fig. 6). Symmetric and asymmetric forms of vibrations also occur in both cases.

6. Conclusions

From the investigations carried out it can be concluded that the efficiency of a perforated disk as a means of reducing the outlet noise is limited by the supply pressure range dependence on η. Fig. 22 is a plot of values of $\overline{p}_a$ from Figs. 14 and 15 that correspond to the beginning of a steep rise of *SPL*, while the continuous line denotes the calculated values of $\overline{p}_a$ that correspond to $\overline{p}_{as} = 0.48$ (broken line in Fig. 21a), i.e. $M_g = 1.08$. The values of $\overline{p}_a$ from Fig. 21b and c, that correspond to the other number of holes, differ only insi-

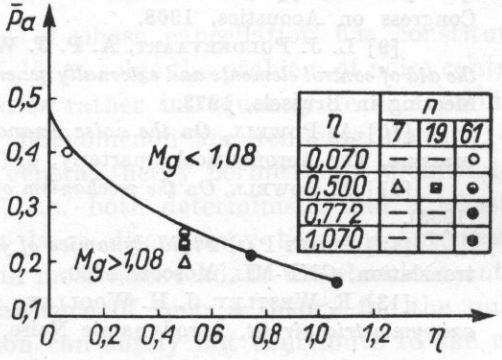

Fig. 22. $\overline{p}_a$ as a function of η for a perforated disk (corresponding to a dynamic *SPL* increase in Figs. 14 and 15)

gnificantly, as described by formula (29). It can be seen that an increase in noise occurs after the formation of the cell structure in a coalesced jet. It is, therefore, desirable that $\overline{p}_a$, for a given η, should always be within the region of efficient operation of the disk, i.e. $M_g < 1.08$. On the other hand, it was found that the lowest level *SPL* occurred when $n = 61$, corresponding to $\eta = 0.5 - 0.8$; thus, the use of higher η can be justified only when there the

the highest supply pressure occurs. It is known, that the *SPL* decreases as the number of holes in the disk [5] increases, but, at the same time, the measurements show that the supply pressure at which the *SPL* of the disk becomes equal to the *SPL* of the nozzle does not depend on the number of holes.

Thus, when using a perforated disk as a single stage element to reduce outflow noise, it is necessary to select a diameter as small as possible for holes in the disk and to choose a value of η as small as possible, but the value of $\overline{p}_a$ should always remain in the region of efficient operation of the disk.

References

[1] M. G. Davies, D. E. S. Oldfield, *Tones from a choked axisymmetric jet*, Acoustics, **12**, 4 (1962).

[2] M. J. Fisher, P. A. Lush, M. H. Bourne, *Jet noise*, Jour. of Sound and Vibr., **28** (3), 563-585 (1973).

[3] D. R. Glass, *Effects of acoustic feedback on the spread and decay of supersonic jets*, AIAA Jour., **6**, 10 (1968).

[4] A. G. Hammitt, *The oscillation and noise of an overpressure sonic jet*, JASA, **28**, 9 (1961).

(5) W. M. Jungowski, A. P. Szumowski, *Perforated disk as an element that reduces the outlet noise*, Archiwum Akustyki, **9**, 3, 339-360 (1974) (in Polish).

[6] E. S. Love, C. E. Grigsby, L. P. Lee, M. J. Woodling, *Experimental and theoretical studies of axisymmetric free jets*, NASA, TR, R-6, 1959.

[7] W. M. Mamin, A. W. Rimskij-Korsakow, *Some properties of radiation of discrete tone by supersonic air-jet*, VII Wsiesojuznaja Akusticzeskaja Konferencja po Fiziczeskoj i Techniczeskoj Akustikie, 1971, Sbornik Dokładow, Leningrad 1973 [in Russian].

[8] L. J. Poldervaart, A. T. Vink, A. P. J. Wijnands, *The photographic evidence of the feedback lopp of a two-dimensional screeching supersonic jet of air*, The 6th International Congress on Acoustics, 1968.

[9] L. J. Poldervaart, A. P. J. Wijnands, L. Bronkhorst, *Aerosonic games with the aid of control elements and externally generated pulses*, Proceedings of the AGARD specialist Meeting in Brussels, 1973.

[10] A. Powell, *On the noise emanating from a two-dimensional jet above the critical pressure*, The Aeronautical Quarterly, **4**, (1953).

[11] A. Powell, *On the mechanism of choked jet noise*, Proc. Phys. Soc., **66**, PT, 12-B (1953).

[12] Shih-i Pai, *Fluid dynamics of jets*, D. Van Nostrand Comp. Inc., 1955, Russian translation, GNF-ML, Moscow 1960.

[13] R. Westley, J. H. Woolley, *An investigation of the near noise fields of a choked axi-symmetric air jet*, Aerodynamic Noise, Proc. of AFOSR-UTIAS Symposium, 1968.

Received on 15th October 1975